(Manuscript for the Fritz Ursell Retirement Meeting, 29-30 March 1990)

THE APPROXIMATION OF FREE-SURFACE GREEN FUNCTIONS

By J. N. Newman

Department of Ocean Engineering
Massachusetts Institute of Technology
Cambridge, MA 02139, USA

As an aspiring student of naval architecture I was frustrated by free-surface Green functions until Fritz Ursell came to my rescue. His analytical expertise was matched by his patience in teaching me the mathematical subtleties of hydrodynamics. In the subsequent three decades he has continued to offer generous assistance whenever an integral or expansion seemed to present insurmountable difficulties. It is a great pleasure to participate in this meeting honouring Professor Ursell.

Abstract

The evaluation of three-dimensional free-surface Green functions is discussed, with emphasis on the use of multivariate economized polynomial approximations. When applicable these provide fast algorithms with controlled accuracy, greatly improving the efficiency and robustness of the computations relative to direct evaluations based on numerical integration. The general method is described, and applied in a relatively simple example involving a periodic array of Rankine sources. More complicated algorithms are described for the free-surface Green function in both the frequency- and time-domains, with the form of the approximations guided by asymptotic expansions. Special attention is given to the large-time asymptotics of the finite-depth impulsive Green function, where the advancing wave front is related to the square of the Airy integral.

1. Introduction

In boundary-value problems for the velocity potential exterior to a floating or submerged body, with a linearized free-surface condition and appropriate radiation condition at infinity, the solution may be derived from Green's theorem. An alternative approach for simple body shapes is to use multipole expansions. The fundamental solution in either case is the source potential which satisfies the free-surface condition, *i.e.* the free-surface Green function.

The principal free-surface Green functions are collected in analytic form by Wehausen & Laitone (1960). Typically these are defined by integral representations, which can be interpreted as transforms in wavenumber space over the domain of the free surface. Most applications are in the frequency domain, where the time-dependence is harmonic with a prescribed frequency ω. The corresponding integrands are oscillatory and include poles at the roots of the plane-wave dispersion relation. Direct numerical integration is inefficient, particularly if the source and field point are close to the free surface.

The first useful computations of the simplest two-dimensional free-surface Green function were presented by Fritz Ursell in his classical paper on the oscillatory motions of a floating circular cylinder (Ursell, 1949). A modified multipole technique was devised with 'wave-free' higher-order multipoles; as a result the only computations required of the free-surface integral were for the source itself, with the source-point at the origin. The same method was used by Havelock (1955) for the analogous three-dimensional problem of a floating hemisphere.

Today it is routine to solve three-dimensional radiation/diffraction problems with $O(10^3)$ discretized panels on the body surface, involving $O(10^6)$ evaluations of the Green function for each frequency. Including only the computations performed in our group at MIT we estimate that 10^{10} evaluations of the frequency-domain Green function have been made in the past two years. Clearly such a level could not be achieved without using special algorithms to evaluate these functions.

From the computational standpoint there are important analogies between free-surface Green functions and Bessel functions. Both can be defined by integral representations and evaluated by quadratures, with a minimum of programming effort, but the computing time is excessive and the robustness is questionable if the argument is large. A suitable combination of the ascending power series and asymptotic expansion provides better algorithms for evaluating, say, the Bessel function $J_0(x)$, but this strictly analytic approach is not without problems. To compute J_0 with an absolute accuracy of 6 decimals requires ten terms in the ascending series, for $|x| \leq 5$, and eleven terms in the asymptotic expansion for the complementary domain $|x| \geq 5$. One significant digit is lost in the ascending series, hence single-precision arithmetic is marginal. Results with increased accuracy are more difficult to obtain, and on a typical computer with 16-17 decimals accuracy in double-precision arithmetic 4-5 decimals are lost due to cancellation errors near the optimum partition. These difficulties can be overcome, and greater computational efficiency can be achieved, if the analytic expansions are replaced by more effective approximations such as truncated Chebyshev expansions or the equivalent economized polynomials.

In evaluating free-surface Green functions three obstacles stand in the way of more efficient approaches: (1) the functions to be evaluated depend on two or three physical coordinates, and usually on additional parameters, all of which may take a large range of values; (2) the user community is small, and (3) there is no compendium of analytic knowledge analogous to Watson's treatise!

Notwithstanding these obstacles, the application of numerical approximations to free-surface Green functions can lead to substantial improvements in computational efficiency

and robustness. As with the simpler Bessel functions, it is vital to separate singularities and persistent oscillations from the slowly-varying residuals or factors. In this respect analytic knowledge is essential, and the most progress has been achieved where we have a comprehensive understanding of the singular features.

My first work in this area was devoted to the three-dimensional frequency-domain Green function, where practical applications abound and the mathematical difficulties are minimal. Emboldened by the success resulting from *ad hoc* combinations of analytic expansions and multivariate polynomial approximations, I considered some aspects of the steady translating Green function, important in the wave-resistance of ships, and also the time-domain impulsive Green function. The results are described in three references (Newman, 1985a,b,1987). Motivated by the need to further reduce computational costs, particularly on vector computers such as the Cray, I have returned to this topic recently with a more heavy-handed reliance on polynomial approximations and less use of analytic expansions except for guidance in the form of the approximations.

Various methods of approximation are available, but I prefer the use of multivariate Chebyshev expansions which lead to economized polynomials with near minimax accuracy or 'equal-ripple' errors. Algorithms for determining the polynomial coefficients, outlined in Newman (1987), are extensions of the procedure for approximating a function of a single real variable by an economized polynomial.

The numerical technique used to derive the polynomial approximations is described in §2. In §3 a simple periodic array of Rankine sources is analysed to illustrate the utility of the method. In this case a single approximation subdomain is sufficient to complement the more familiar Fourier series. Approximations of the frequency-domain Green functions are described in §§4-5 for infinite and finite fluid depths, respectively. For these functions the analytic and asymptotic properties are well established, and attention is focussed on more unified and efficient approximations which are suitable for vectorization.

In §§6-7 the analogous Green functions are considered for impulsive motion in the time domain. Special attention is given to the large-time asymptotics, which are prerequisites to the development of corresponding numerical approximations. In the infinite-depth case the method of steepest descents is utilized in a straightforward manner. The asymptotics are more complicated in a fluid of finite depth, where the front which advances with the limiting group velocity separates the oscillatory waves from an exponentially small disturbance far ahead. The transition between these two regions suggests an asymptotic expansion in terms of Airy integrals using the method of Chester, Friedman & Ursell (1957), as in the analysis of the two-dimensional Cauchy-Poisson problem by Whitham (1974). However this approach is not directly applicable in the three-dimensional case, where we show that the wave front is described to leading order by the *square* of the Airy integral.

In the concluding §8 the use of polynomial approximations is compared with other computational approaches based on table look-up and interpolation. Progress is briefly noted on the analysis of ships, where a steady forward velocity is superposed.

2. Polynomial approximation

Given a function $F(x,y)$ which is regular in the domain $|x| \leq 1$, $|y| \leq 1$, a Chebyshev expansion may be assumed in the form

$$F = \sum_{m=0}^{\infty} \sum_{n=0}^{\infty} c_{m\,n} T_m(x) T_n(y) \qquad (1)$$

where T_m is the Chebyshev polynomial. Since F is regular the sequence of coefficients $c_{m\,n}$ will converge to zero and the series may be truncated to yield any desired degree of accuracy. The extension to three or more variables is straightforward.

For computational convenience the result can be converted to an ordinary polynomial. Gradients of the Green function may be evaluated using term-by-term differentiation of the polynomials, but extra accuracy is necessary in the approximations to offset the loss inherent in differentiation. Nested multiplication permits the polynomials to be evaluated with one floating-point multiplication and addition per term. Derivatives can be evaluated concurrently, with the same computational cost, by using a simple extension of the nested-multiplication algorithm.

The requirement that F be 'regular' is not strict. Weak singularities such as $x^k \log x$ can be tolerated if k is sufficiently large. This pragmatic consideration is significant if we lack a complete understanding of the singularity, or if a simpler representation is expedient from the computing standpoint. Generally the suitability of F for representation in the form (1) can be judged by superficial examination of the coefficients. One learns from experience to determine the types of singularities which have been overlooked, or incorrectly removed, by the resulting sequence of coefficients. Table 1 shows a 'good' matrix of Chebyshev coefficients, corresponding to the economized polynomial coefficients $a_{m\,n}^{(+)}$ in equation (7) and Table 2.

n	$m=0$	$m=1$	$m=2$	$m=3$	$m=4$
0	0.01207372	0.02464014	0.00025322	0.00000300	*0.0000004*
1	-0.01393953	-0.00178218	-0.00005811	-0.00000146	*-0.0000008*
2	0.00014993	0.00005214	0.00000332	*0.0000001*	*0.00000000*
3	-0.00000242	-0.00000140	*-0.0000001*	*-0.00000001*	*-0.00000000*
4	*0.00000005*	*0.00000004*	*0.00000001*	*0.00000000*	*0.00000000*

Table 1 – Coefficients $c_{m\,n}$ of the Chebyshev expansion (1) for the source array G_+ defined in (6). Coefficients with an absolute value less than 10^{-6} are italicized.

The discrete orthogonality relation is convenient for computing the Chebyshev coefficients. An accurate subroutine is essential for the evaluation of F, ideally with several more decimals precision than is needed in the final approximation. Efficiency is not important, since the subroutine is used only to construct the polynomial coefficients. Numerical integration of the Green functions is appropriate in this context, provided an adaptive method such as Romberg quadrature is employed to assure the required degree of accuracy. When

using the discrete orthogonality relation it is necessary to truncate the Chebyshev expansions *a priori* at some appropriate upper limits $m = M$, $n = N$ which exceed the ultimate degrees of truncation based on the economization tolerance. In practice $M = N = 8$ or 16 are convenient choices. A preliminary examination of the convergence will indicate if these are not sufficiently large, in which case it may be more appropriate to subdivide the domain of approximation (or reconsider the singular features of F!) rather than increasing M or N.

The accuracy required for approximations of Green functions is an important practical issue. For applications with integrated surface distributions there is no point in preserving the relative accuracy locally at points where the function is small. The present discussion is in the context of approximations with 6-7 decimals absolute accuracy, the maximum consistent with single-precision arithmetic on most computing systems. Polynomial approximations with greater or lesser accuracy may be derived by the same techniques, and require larger or smaller numbers of coefficients, respectively.

It might be argued that 6-7 decimals are unnecessary for engineering applications, where precision greater than 2-3 decimals in the final results usually is irrelevant. On the other hand, since the gradient of the Green function is required for the coefficient matrix, and the condition number of the resulting linear system is frequently $O(100)$, 6-7 decimals are not excessive. Furthermore, validation of programs and numerical methods depends on convergence tests and comparisons with benchmarks, which should be made to a higher degree of accuracy than is required in engineering practice.

The algorithm for truncating the Chebyshev expansion must be considered together with the desired accuracy. Since $|T_m| \leq 1$ the contribution from each separate term is bounded by $|c_{mn}|$. The simplest choice is to ignore any coefficient with magnitude less than a prescribed tolerance. A more conservative criterion is to sum the absolute values of all coefficients backwards from large upper limits, and ignore all terms if the sum itself is less than the tolerance. In one dimension this process is unique, but in multiple dimensions there is some flexibility. In Table 1, for example, the absolute sum of the italicized terms is 4.6×10^{-7}. Setting all of these terms equal to zero will therefore result in a maximum economization error of the same amount. On the other hand, if a tolerance of 4.0×10^{-7} is imposed, either the coefficient c_{23} or the coefficient c_{32} could be removed, but not both. This flexibility in truncation can be exploited to preserve the form of the polynomial approximations in different subdomains, *i.e.* the same number of coefficients is retained in each column and each row of the truncated matrix. This is an important practical feature from the programming standpoint since the same code may be used for every subdomain if the coefficients are stored in a common array.

3. Array of Rankine image sources

In two limiting cases the free-surface boundary condition reduces to a homogeneous Neumann or Dirichlet condition. These correspond respectively to $\omega = 0, \infty$ in the frequency domain, and $t = \infty, 0$ for impulsive motion in the time domain. For a fluid of infinite depth the solution is simply a Rankine source $1/r$ together with its image of the same or opposite sign, above the plane of the free surface. For finite depth the solution can be constructed from a pair of periodic source arrays

$$G_{\pm}(R,z) = [R^2 + z^2]^{-\frac{1}{2}} + \sum_{\substack{n=-\infty \\ n \neq 0}}^{\infty} (\pm)^n \left\{ [(R^2 + (z+2n)^2]^{-1/2} - \frac{1}{2|n|} \right\} \tag{2}$$

where the two alternatives correspond respectively to Neumann and Dirichlet conditions on the boundary $z = 1$. To secure convergence in the former case a constant has been subtracted from each term. The cylindrical coordinates (R, z) are defined with the array on the z-axis and the normalized spacing equal to two. The function G_- can be derived by forming the difference between two functions G_+, with an appropriate shift of the origin, but it is useful to treat these alternative cases separately.

Fourier series are easily derived, as in Gradshteyn & Ryzhik (1965), §8.526. The resulting expressions are

$$G_+ = 2 \sum_{m=0}^{\infty} \cos(m\pi z) K_0(m\pi R) - \gamma - \log(\tfrac{1}{4}R) \tag{3a}$$

$$G_- = 2 \sum_{m=0}^{\infty} \cos((m+\tfrac{1}{2})\pi z) K_0((m+\tfrac{1}{2})\pi R) + \log 2 \tag{3b}$$

Here K_0 is the modified Hankel function and $\gamma = 0.577...$ is Euler's constant. These series converge rapidly, except for small values of R. If $R > 1$ a maximum of six terms is sufficient to give 7-8 decimals accuracy.

The objective here is to complement (3) with alternative algorithms which are effective when $R \leq 1$. Since both functions are periodic in z, with obvious symmetry or anti-symmetry relations about the planes $z = 0, \pm 1, \pm 2, \ldots$, it may be assumed hereafter that $0 \leq z \leq 1$.

If the Hankel transform for the inverse square-root is substituted for each term in (2) the series can be summed to give the integral representations

$$G_{\pm} = [R^2 + z^2]^{-\frac{1}{2}} \pm \int_0^{\infty} \exp(-k) \begin{pmatrix} \mathrm{csch} k \\ \mathrm{sech} k \end{pmatrix} [\cosh(kz) J_0(kR) - 1] dk \tag{4}$$

These integrals converge if $|z| < 2$. For sufficiently small values of R and z the integrand can be expanded in even powers of these coordinates, and integrated term-by-term. After using integral representations for the (Riemann) zeta function ζ, it follows that

$$G_{\pm} = [R^2 + z^2]^{-\frac{1}{2}}$$

$$+ \sum_{\substack{m=0 \\ m+n\neq 0}}^{\infty} \sum_{n=0}^{\infty} (-)^m \frac{(2m+2n)!}{(m!)^2(2n)!} \begin{pmatrix} 1 \\ 1 - 2^{-2m-2n} \end{pmatrix} \varsigma(2m+2n+1) (\tfrac{1}{4}R)^{2m} (\tfrac{1}{2}z)^{2n} \qquad (5)$$

An equivalent result for G_+ has been derived by Breit (1990) using Taylor expansions.

As the basis for more efficient computational algorithms, the adjacent singularities in (2) corresponding to the terms $n = \pm 1$ are subtracted from the integral representation to accelerate the convergence as $k \to \infty$:

$$G_{\pm} = [R^2 + z^2]^{-\frac{1}{2}} \pm [R^2 + (z+2)^2]^{-\frac{1}{2}} \pm [R^2 + (z-2)^2]^{-\frac{1}{2}} \mp 1$$

$$\pm \int_0^{\infty} \left\{ \exp(-k) \begin{pmatrix} \operatorname{csch} k \\ \operatorname{sech} k \end{pmatrix} [\cosh(kz) J_0(kR) - 1] \right. \qquad (6)$$

$$\left. - 2\exp(-2k) \cosh(kz) J_0(kR) \right\} dk$$

In the domain $(0 \le R \le 1,\ 0 \le z \le 1)$ these integrals define regular functions, which can be approximated by economized polynomials. The results take the form

$$G_{\pm} \simeq [R^2 + z^2]^{-\frac{1}{2}} \pm [R^2 + (z+2)^2]^{-\frac{1}{2}} \pm [R^2 + (z-2)^2]^{-\frac{1}{2}} \mp 1$$

$$+ \sum_{m,n} a_{mn}^{(\pm)} R^{2m} z^{2n} \qquad (7)$$

where the coefficients $a_{mn}^{(\pm)}$ are given in Tables 2 and 3. These coefficients have been obtained in the manner outlined in §2, based on Chebyshev expansion of the functions defined by the integrals in (6), and neglect of the Chebyshev coeficients with magnitude smaller than 10^{-9}. The resulting polynomial approximations are accurate to about 8 decimals. (Table 1 shows the Chebyshev coeficients corresponding to a_{mn}^{+}.)

The utility of this approach is that the slowly-convergent series (2) (excluding the three dominant terms $n = -1, 0, 1$) are approximated by polynomials which can be evaluated with 21 floating-point multiplications/additions. Similar approximations can be derived directly from (4) or (5), without subtracting the adjacent singularities in (6), but the convergence of the Chebyshev expansions is reduced and more terms are required to achieve the same accuracy.

n	$m=0$	$m=1$	$m=2$	$m=3$	$m=4$
0	0.00000000	-0.02525711	0.00086546	-0.00004063	0.00000193
1	0.05051418	-0.00692380	0.00073292	-0.00006636	0.00000398
2	0.00230838	-0.00097875	0.00020597	-0.00003333	0.00000524
3	0.00012934	-0.00010879	0.00003965	-0.00000891	
4	0.00000913	-0.00001270	0.00000466		

Table 2 – Coefficients $a_{mn}^{(+)}$.

n	$m=0$	$m=1$	$m=2$	$m=3$	$m=4$
0	0.00000000	0.01230716	-0.00065341	0.00003603	-0.00000182
1	-0.02461428	0.00522739	-0.00065004	0.00006286	-0.00000386
2	-0.00174290	0.00086822	-0.00019543	0.00003259	-0.00000519
3	-0.00011463	0.00010319	-0.00003877	0.00000882	
4	-0.00000870	0.00001243	-0.00000460		

Table 3. – Coefficients $a_{mn}^{(-)}$.

4. Frequency domain – infinite depth

If the time-dependence is harmonic, with frequency ω, the Green function is defined by the expression

$$G = 1/r + 1/r_1 + \int_0^\infty \frac{k+K}{k-K} e^{kz} J_0(kR)\,dk$$
$$= 1/r + KF(KR, |Kz|) - 2\pi i K e^{Kz} J_0(KR) \tag{8}$$

(Wehausen & Laitone, 1960, eq. 13.17). Here $1/r_1$ is the potential of the image source above the free surface, $K = \omega^2/g$ is the wavenumber with g the gravitational acceleration constant, and (R, z) are cylindrical polar coordinates with z positive upwards and the origin at the image source point. The time-dependent factor $\exp(i\omega t)$ is assumed, and the contour is deformed above the pole in accordance with the radiation condition. The essential task is to evaluate the function $F(X, Y)$ throughout the quadrant ($0 \le X < \infty$, $0 \le Y < \infty$), excluding the singular point at the origin.

Newman (1985a) describes a set of comprehensive but disjoint algorithms for this purpose. Different analytic expansions are used in four subregions around the perimeter of the (X, Y) quadrant, complemented by economized polynomials in the interior region where the analytic expansions are not efficient. The resulting subroutine is robust, and efficient on a serial computer, but the variety of diverse algorithms and associated branches precludes effective use on a vector machine such as the Cray.

Adopting a more systematic numerical approach, we use the analytic expansions only as guides for removal or suppression of the singular or oscillatory features of $F(X, Y)$, and approximate the remainder in all cases with economized polynomials. For this purpose the quadrant is subdivided into four rectangular domains with partitions at $X = 3$ and $Y = 4$. From the expansions given by Newman (1985a) four corresponding approximations can be inferred:

Region 1 ($0 \le X \le 3$, $0 \le Y \le 4$):

$$F(X,Y) = e^{-Y}\Big\{-2J_0(X)\log(R+Y) - \left[\pi Y_0(X) - 2J_0(X)\log(x)\right] + Rf(X^2, Y)\Big\}$$

Region 2 ($3 \le X < \infty$, $0 \le Y \le 4$):

$$F(X,Y) = -2\pi e^{-Y} Y_0(X) + f(X^{-1}, Y)$$

Region 3 ($0 \le X \le 3$, $4 \le Y < \infty$):

$$F(X,Y) = f(X^2, Y^{-1})$$

Region 4 ($3 \le X < \infty,\ 4 \le Y < \infty$):

$$F(X,Y) = -2\pi e^{-Y} Y_0(X) + \sum_{n=0}^{2} n! P_n(\cos\theta) R^{-(n+1)} + f(X^{-1}, Y^{-1})$$

Here J_0, Y_0 denote the Bessel functions, R, θ are spherical coordinates with $Y = R\cos\theta$, and $P_n(\cos\theta)$ is the Legendre polynomial. In each region f denotes a (different) residual function of the two indicated variables, to be approximated by an economized polynomial.

The success of this approach depends on the extent to which the residual function f is slowly-varying. In Region 1 the logarithmic singularity is represented exactly, and the remainder f is strictly regular. Similarly in Region 3, the asymptotic behaviour of the integral in (8) can be used to confirm the assumed form. However in Regions 2 and 4 the extra terms are somewhat *ad hoc*. A more correct form would replace $2Y_0$ by the sum $Y_0 + \mathbf{H}_0$ where $\mathbf{H}_0$ is the Struve function, but since the difference $Y_0 - \mathbf{H}_0$ is algebraic in X^{-1} it is unnecessary to evaluate $\mathbf{H}_0$. Including the three-term spherical-harmonic series in Region 4 reduces the variation of the residual function.

In principle a single polynomial approximation is feasible in each domain, but to avoid excessive numbers of terms it is necessary to introduce additional partitions. Numerical experimentation indicates that a total of 48 subdomains are effective, separated by partitions at $X = 3, 3.75, 5, 7.5, 15$ and $Y = 1, 2, 3, 4, 5\frac{1}{3}, 8, 16$. A total of 31 terms in each economized double-polynomial is suitable to yield an absolute accuracy of 6 decimals for each subdomain. Aside from the relatively simple extra terms required in Regions 1,2, and 4, the computation of F is reduced to the evaluation of this polynomial. A total of $48 \times 31 = 1488$ polynomial coefficients must be stored in the program.

From the programming standpoint the complications of a large number of subdomains can be minimized by using polynomials of the same degree, and storing the coefficients sequentially in a large array. A single block of nested-multiplication code can then be used for all cases. This code can be vectorized, thus permitting the simultaneous evaluation of a large number of Green functions in one subroutine call; on a Cray this procedure reduces the computational cost of each Green-function evaluation by a factor of 5-10.

5. Frequency domain – finite depth

For a fluid of constant depth h with vanishing normal velocity on the bottom, the extension of (8) is given by

$$G = 1/r + 1/r_2 + 2\int_0^\infty \frac{k+K}{k\sinh(kh) - K\cosh(kh)} e^{-kh} \cosh(k(z+h))\cosh(k(\zeta+h))J_0(kR)dk \tag{9}$$

(Wehausen & Laitone, 1960, eq. 13.18). Here (R,z) is a cylindrical coordinate system with vertical axis, the fluid domain is $(-h \le z \le 0)$, the source point is at $(0,\zeta)$, and $1/r_2$ is the potential of the image source beneath the bottom. As in the infinite-depth case the appropriate contour of integration is above the pole.

An eigenfunction expansion analogous to (3) (Wehausen & Laitone, 1960, eq. 13.19) can be used effectively for computations unless the ratio R/h is small. The procedure adopted by Newman (1985a) is based on a partition at $R/h = 1/2$. For $R/h \ge 1/2$ a maximum of 12 terms in the eigenfunction expansion gives an accuracy of 6 decimals. In the complementary domain $R/h \le 1/2$ the hyperbolic addition theorem is used to express the Green function, initially dependent upon four nondimensional parameters $(R/h, z/h, \zeta/h, Kh)$, as the sum of two auxiliary functions L which depend on only three parameters $(X = R/h, V = |z/h \pm \zeta/h|, Kh)$. (The function L involves an integral similar to that in (9) but with $\zeta = -h$; the same decomposition is used in §7.) The convergence of the integral representation for L can be accelerated by subtracting two infinite-depth integrals of the form (8). The difference is a regular function of the three parameters which can be approximated by *triple* economized polynomials (except in the limit $Kh \to 0$ where a logarithmic singularity must be accounted for). With three subdomains in Kh 6 decimals accuracy requires about 300 terms, but in the usual applications involving many values of the source and field points for the same frequency and depth, the polynomials in Kh can be evaluated at the outset, leaving only 33 terms for the polynomials in terms of (X,V). The resulting algorithm for G requires two evaluations of this polynomial, and four evaluations of the infinite-depth Green function.

As in the infinite-depth case, recent improvements have been made in these algorithms. The eigenfunction expansion is used only in the domain $X \ge 1$, thereby halving the maximum number of terms required. In the domain $(0 \le X \le 1)$ two evaluations of the auxiliary function $L(X,V,Kh)$ are used, as before, but the domain of the vertical coordinate is subdivided at $V = 1$ and the infinite-depth limit of the integrand is subtracted only when $V \le 1$. To cover the extended domain $(0 \le X \le 1)$ more partitions are required in the parameter Kh, and the total number of stored coefficients increases to about 8000. For a fixed value of Kh the Green function is evaluated from two polynomials with 32 terms in each, and from only one or two evaluations of the infinite-depth function. In addition to a modest reduction in serial computing time, the resulting algorithms are more amenable to vectorization and lead to similar Cray performance as noted for the infinite-depth case.

6. Time domain – infinite depth

For a fluid of infinite depth the potential of an impulsive source with strength $\delta(t)$ is

$$G = \frac{\delta(t)}{r} - \frac{\delta(t)}{r_1} + 2\int_0^\infty \sqrt{gk}\sin(t\sqrt{gk})e^{kz}J_0(kR)\,dk \tag{10}$$

(Wehausen & Laitone, 1960, eq. 13.49). Here the coordinates are as defined in §4.

It is convenient to use spherical coordinates (r_1, θ), with the angle θ measured from the negative vertical axis, and to nondimensionalize the physical parameters with respect to g and r_1. The variable t is replaced by $\tau = t\sqrt{g/r_1}$. Thus

$$G = \frac{\delta(t)}{r} - \frac{\delta(t)}{r_1} + g^{\frac{1}{2}}r_1^{-\frac{1}{2}}\,\mathrm{Re}\{F(\tau,\theta)\} \tag{11}$$

where

$$\begin{aligned} F &= -2i\int_0^\infty k^{\frac{1}{2}}\exp(ik^{\frac{1}{2}}\tau - k\cos\theta)J_0(k\sin\theta)\,dk \\ &= -4i\int_0^\infty \omega^2\exp(i\omega\tau - \omega^2\cos\theta)J_0(\omega^2\sin\theta)\,d\omega \end{aligned} \tag{12}$$

and the new integration variable is $\omega = k^{1/2}$. The objective is to evaluate (12) in the computational domain $(0 < \tau < \infty,\ 0 \le \theta \le \pi/2)$. The function F is the first-derivative with respect to time of the corresponding integral studied by Newman (1985b).

The integrand of (12) may be expanded in ascending powers of τ and integrated term-by-term to give the spherical-harmonic expansion

$$F = -2i\sum_{n=0}^{\infty}\frac{(i\tau)^n}{n!}\Gamma(\tfrac{1}{2}n + \tfrac{3}{2})P_{\frac{1}{2}n+\frac{1}{2}}(\cos\theta) \tag{13}$$

where P_ν is the Legendre function. This expansion is uniformly convergent.

For large values of τ asymptotic expansions can be derived in a similar but more complete manner relative to those outlined by Newman (1985b). For this purpose (12) is decomposed in the form

$$F = f_0 + f_1 + f_2 \tag{14}$$

where

$$f_0 = -4i\int_0^{\frac{1}{2}i\tau} \omega^2\exp(i\omega\tau - \omega^2\cos\theta)J_0(\omega^2\sin\theta)\,d\omega \tag{15}$$

$$f_{1,2} = -4i\int_{\frac{1}{2}i\tau}^\infty \omega^2\exp(i\omega\tau - \omega^2\cos\theta)H_0^{(1,2)}(\omega^2\sin\theta)\,d\omega \tag{16}$$

and $H_0^{(1,2)}$ denotes the Hankel functions $J_0 \pm iY_0$.

The integral f_0 can be expanded using Watson's Lemma, with the result

$$f_0 \simeq -4 \sum_{n=0} \frac{(2n+2)!}{n!} \tau^{-2n-3} P_n(\cos\theta) \tag{17}$$

The error in (17) is of order $\exp(-\frac{1}{4}\tau^2)$.

Let θ_0 denote a fixed angle such that $0 < \theta_0 < \frac{1}{2}\pi$. For $\theta < \theta_0$ the remaining integrals $f_{(1,2)}$ are exponentially small, and (17) is a complete asymptotic expansion of $F(\tau,\theta)$ for large τ.

For $\theta > \theta_0$ the argument of the Hankel functions in (16) is $O(\tau)$ or larger, provided the contour of integration is restricted so that $|\omega| \geq \frac{1}{2}\tau$. Thus these functions may be evaluated from the asymptotic expansions

$$H_0^{(1,2)}(\omega^2 \sin\theta) \simeq \exp(\pm i(\omega^2 \sin\theta - \pi/4)) \sqrt{\frac{2}{\pi\omega^2 \sin\theta}} \sum_{n=0} (\pm i)^n c_n (\omega^2 \sin\theta)^{-n} \tag{18}$$

where

$$c_n = \frac{[\Gamma(n+\frac{1}{2})]^2}{\pi 2^n n!}$$

Substituting (18) in (16) gives the expansions

$$f_{(1,2)} \simeq \frac{-4i}{\sqrt{2\pi \sin\theta}} e^{\mp i\pi/4} \sum_{n=0} (\mp i)^n c_n$$

$$\int_{\frac{1}{2}i\tau}^{\infty} \omega \exp(i\omega\tau \pm i\omega^2 \sin\theta - \omega^2 \cos\theta)(\omega^2 \sin\theta)^{-n} d\omega \tag{19}$$

The contours of integration in these two integrals may be deformed, in the half-plane $\mathrm{Re}(\omega) > 0$, with the upper limit a point at infinity in the sector $(-\pi/4 \pm \theta/2, \pi/4 \pm \theta/2)$. In each integral there is one saddle point, at $\omega_{(1,2)} = \frac{1}{2}\tau i e^{\pm i\theta}$. For the integral f_1 this saddle point is in the second quadrant and can be ignored. It follows that f_1 is exponentially small for all values of θ. For the integral f_2 the saddle point is in the first quadrant, and it is appropriate to deform the contour of integration to pass through this point. To clarify the analysis a local integration variable $v = ie^{-i\theta/2}(\omega/\omega_2 - 1)$ can be used to give

$$f_2 \simeq \frac{-4}{\sqrt{2\pi \sin\theta}} \exp(-\tfrac{1}{4}\tau^2 e^{-i\theta} + i\theta/2 + i\pi/4) \sum_{n=0} i^n c_n \omega_2^{2-2n} (\sin\theta)^{-n}$$

$$\int_{-2\sin(\theta/2)}^{\infty} \exp(-\tfrac{1}{4}\tau^2 v^2)(1 - ie^{i\theta/2}v)^{1-2n} dv \tag{20}$$

After expanding the last factor in the integrand about $v = 0$, replacing the lower limit by $-\infty$, and integrating term-by-term, the desired asymptotic expansion is obtained in the form

$$f_2 \simeq \frac{-4i}{\sqrt{2\sin\theta}} \exp(-\tfrac{1}{4}\tau^2 e^{-i\theta} - i\theta/2 + i\pi/4) \sum_{n=0} i^n (\sin\theta)^{-n} \sum_{m=0} d_{nm}\, \omega_2^{1-2m-2n} e^{-im\theta} \quad (21)$$

where $d_{00} = 1$, $d_{0m} = 0$ for $m > 0$, and for $n \geq 1$

$$d_{nm} = c_n \frac{(2m+2n-2)!}{(2n-2)!2^{2m}m!}$$

If the substitution $\omega_2 = \frac{1}{2}i\tau e^{-i\theta}$ is made in (21) the result is a descending series in odd powers of the (large) parameter τ. Since the terms with $m+n \equiv N-1$ are of order τ^{3-2N}, this double series may be summed in a triangular manner to any desired order N.

When $\theta = \pi/2$, F can be expressed in terms of products of Bessel functions of argument $\tau^2/8$ and orders $\pm\frac{1}{4}$ and $\pm\frac{3}{4}$, following the corresponding analysis of the Cauchy-Poisson problem (Wehausen & Laitone, 1960; see also Magee & Beck, 1989). For large values of τ these products can be expressed, by the trigonometric addition theorems, as the sum of a slowly-varying descending asymptotic series plus an oscillatory component, analogous respectively to (17) and (21).

Our first subroutine for the evaluation of this Green function used the three analytic expansions (13,17,21). The principal problem in this approach is that the partition between the ascending series (13) and asymptotic expansions (17,21) must be at a relatively large value of τ, about $\tau = 9$ to obtain 6 decimals accuracy in the asymptotic expansions, but this is too large for efficient use of (13).

In our next subroutine we subdivided the (τ, θ) domain into 27 rectangles and approximated the difference between F and the asymptotic expansion (21) of 'optimum order' N in each subdomain by a two-dimensional economized polynomial. The optimum order N is defined to minimize the number of nonzero coefficients in the economized polynomial. Six decimals accuracy is achieved with an average of 30 nonzero polynomial coefficients in each subdomain. This approach, with the number of terms in the asymptotic expansion 'optimized' between 0 and 6, appeared to be an elegant combination of analytical and numerical techniques, and it led to a significant improvement in terms of computational speed. However the $N = 6$ steepest-descent evaluation (involving a total of 21 complex terms) required substantial time.

The third subroutine developed for this Green function reflects the experience with the more 'heavy-handed' use of economized polynomials in the frequency domain. The objective was to restrict the order of the steepest-descent expansion to $N = 2$, without sacrificing accuracy. This has been achieved by using a finer rectangular grid with a total of 240 subdomains, defined with partitions at $\tau = 2(.5)13$ and $\cos\theta = 0.1(.1)0.9$.

In each subdomain the economized polynomial requires 32 coefficients, hence a total of 7680 coefficients must be stored. The polynomial is augmented by the steepest-descent expansion with $N = 2$ in the subdomains where $\tau > 4$ and $\cos\theta < .4$. The coding is similar to that described in the frequency domain, and vectorization is feasible on the Cray. (For the Green function and its two first-derivatives, the time required on a VAX 11-750 is about 1 millisecond; on the Cray with vectorization implemented the corresponding time is about 1 microsecond. These times are somewhat faster than we have achieved for the frequency-domain Green function.)

In deriving the Chebyshev expansion coefficients F is evaluated by a combination of four separate algorithms: (a) for small or moderate values of τ (13) is used; (b) for very large values of τ the asymptotic expansions (17) and (19) are used; (c) for intermediate values of τ, and $\cos\theta > \frac{1}{2}$, (12) is integrated numerically along the real axis; and (d) for intermediate values of τ and smaller values of $\cos\theta$ the integral is evaluated numerically in the complex plane. The numerical integration is performed by Romberg quadratures with a convergence tolerance of 10^{-10}.

7. Time domain – finite depth

In a fluid of depth h, the impulsive Green function is represented in the form

$$G = \frac{\delta(t)}{r} + \frac{\delta(t)}{r_2} - 2\delta(t)\int_0^\infty \frac{\exp(-kh)}{\cosh(kh)}\cosh(k(y+h))\cosh(k(z+h))J_0(kR)dk$$

$$+ 2\int_0^\infty \frac{\sqrt{gk\tanh kh}}{\cosh(kh)\sinh(kh)}\sin(t\sqrt{gk\tanh kh}) \qquad (22)$$

$$\cosh(k(y+h))\cosh(k(z+h))J_0(kR)dk$$

(Wehausen & Laitone, 1960, eq. 13.53).

It is convenient to nondimensionalize with respect to the parameters g and h. After defining the variables $X = R/h$, $Y = -\zeta/h$, $Z = -z/h$, $T = t\sqrt{g/h}$, and using the addition theorem for the product of two hyperbolic cosines, G can be expressed in the form

$$G = g^{1/2}h^{-3/2}\{\delta(T)[F_0(X,Y-Z) + F_0(X,2-Y-Z)] \qquad (23)$$

$$+ F(X,Y-Z,T) + F(X,2-Y-Z,T)\}$$

where

$$F_0(X,V) = 1/\sqrt{X^2+V^2} - \int_0^\infty \exp(-k)\mathrm{sech}k\cosh(kV)J_0(kX)dk \qquad (24)$$

and

$$F(X,V,T) = \int_0^\infty \frac{\sqrt{k\tanh k}}{\cosh k\sinh k}\sin(T\sqrt{k\tanh k})\cosh(kV)J_0(kX)dk \qquad (25)$$

The vertical coordinate V is in the range $(0,2)$.

It is straightforward to evaluate $F_0 = G_-(X,V) - \log(2)$ using (3b), (7), and the polynomial coefficients in Table 3.

The efficient evaluation of the time-dependent function F presents a more challenging problem. As in the frequency domain it is useful in some regimes to subtract from (25) the 'infinite-depth limit' F_∞, defined by replacing the hyperbolic functions in (25) by their respective limiting forms for large k. This limit can be evaluated by means of the algorithms described in §6.

For values of the nondimensional time T up to about 10 it is possible to approximate either the function F or the difference $F - F_\infty$ using economized triple polynomials in

the variables X, V, T. Preliminary results have been obtained for the relevant range ($0 \leq V \leq 2$) with subdomains in the X, T space bounded by partitions at integer intervals. For example, for ($6 \leq X \leq 7$) and ($7 \leq T \leq 8$) F can be approximated with about 6 decimals accuracy by a polynomial with 125 terms. In the same domain the difference $F - F_\infty$ can be approximated with 118 terms. The latter function is the appropriate quantity to use for smaller values of X. In applications where the solution proceeds in time steps, the nondimensional time T is constant at each step and for each combination of source and field points a relatively simple polynomial is evaluated. Thus in the last example with 118 terms in the triple polynomial, pre-evaluation with a fixed value of T yields a polynomial in (X, V) with only 31 terms. (This procedure is similar to that described in §5, where T is replaced by Kh.)

Asymptotic expansions are required for larger values of time, to provide guidance in the development of numerical algorithms. As in the analogous treatment of the two-dimensional Cauchy-Poisson problem by Whitham (1974), it is necessary to consider three overlapping domains in relation to the front $X = T$.

Well behind the front, where $X << T$, (25) can be expressed in a form analogous to (14-16). Thus

$$F(X, V, T) = \mathrm{Re}\{f_0 + f_1 + f_2\} \tag{26}$$

where

$$f_0 = -2i \int_0^{i\kappa_0} \frac{\omega}{\sinh 2k} \cosh kV \, e^{i\omega T} J_0(kX) dk \tag{27}$$

$$f_{1,2} = -i \int_{i\kappa_0}^{\infty} \frac{\omega}{\sinh 2k} \cosh kV \, e^{i\omega T} H_0^{(1,2)}(kX) dk \tag{28}$$

and $\omega(k) = \sqrt{k \tanh k}$. The parameter κ_0 may be fixed so that the upper limit in (27) is at an arbitrary point below the first pole on the positive imaginary axis, say $\kappa_0 = \pi/4$.

As in §6, these three integrals contribute, respectively, a slowly-varying asymptotic series, an exponentially small contribution, and a contribution from the saddle point on the real axis.

We begin by considering the function f_0 defined by (27). Since $\omega(k) \simeq k$ is single-valued near the origin it is straightforward to substitute $k = i\kappa$ and $\Omega(\kappa) = -i\omega(k) = \sqrt{\kappa \tan \kappa}$. It follows that

$$f_0 = 2 \int_0^{\kappa_0} \frac{\Omega}{\sin 2\kappa} \cos \kappa V \, e^{-\Omega T} I_0(\kappa X) d\kappa \tag{29}$$

where I_0 is the modified Bessel function of the first kind. Since $T > X$ and $\Omega \geq \kappa$ the integrand of (29) is exponentially small away from the origin. To estimate the contribution near the origin we use the series expansion

$$\Omega = \kappa + \tfrac{1}{6}\kappa^3 + O(\kappa^5) \tag{30}$$

and expand the integrand of (29) in the form

$$f_0 = \int_0^{\kappa_0} \left[1 + \left(\tfrac{5}{6} - \tfrac{1}{2}V^2\right)\kappa^2 - \tfrac{1}{6}T\kappa^3 + O(\kappa^4)\right] e^{-\kappa T} I_0(\kappa X) d\kappa \qquad (31)$$

After replacing the upper limit by ∞ and using the transform

$$\int_0^{\infty} e^{-\kappa T} I_0(\kappa X) d\kappa = (T^2 - X^2)^{-\frac{1}{2}}$$

(and its partial derivatives with respect to T) to evaluate (31) term-by-term, it follows that

$$\begin{aligned} f_0 =& (T^2 - X^2)^{-\frac{1}{2}} \\ &+ \left(\tfrac{5}{6} - \tfrac{1}{2}V^2\right)(2T^2 + X^2)(T^2 - X^2)^{-\frac{5}{2}} - \tfrac{1}{2}T^2(2T^2 + 3X^2)(T^2 - X^2)^{-\frac{7}{2}} \qquad (32) \\ &+ O[T^4(T^2 - X^2)^{-\frac{9}{2}}] \end{aligned}$$

This sequence converges asymptotically, subject to the inequalities $(T - X)^3 >> T >> 1$.

Proceeding to the asymptotics of (28), we note that in the strip $-\frac{1}{2}\pi < \mathrm{Im}(k) < \frac{1}{2}\pi$ adjacent to the positive real axis, the imaginary part of $\omega(k)$ is bounded and has the same sign as $\mathrm{Im}(k)$. From (18) it follows that f_1 can be evaluated along the contour $\mathrm{Im}(k) = \kappa_0$, where the integrand is exponentially small and thus f_1 is of order $e^{-\kappa_0 T}$. For f_2 there is a saddle point on the real axis at the (positive) root of the equation $\omega' = X/T$, where the integrand is locally of order one. At this point the path of steepest descent is along the vector which intersects the real k-axis at an angle $-\pi/4$. Defining the root by k_0 and the corresponding value $\omega_0 = \omega(k_0)$, a procedure similar to that in §6 gives the leading-order approximation

$$\mathrm{Re}(f_2) \simeq 2\sqrt{\frac{\tanh k_0}{|\omega_0''|XT}} \frac{\cosh k_0 V}{\sinh 2k_0} \sin(\omega_0 T - k_0 X) \qquad (33)$$

where ω_0'' is the (negative) second derivative of $\omega(k)$ evaluated at $k = k_0$. An algorithm for extending (33) to higher-order terms can be constructed in a manner analogous to (21), but the analysis is involved. To illustrate this procedure the two leading terms after (33) are derived in the Appendix.

Proceeding in a similar manner ahead of the front, for $X >> T$, the saddle point is on the imaginary axis at $k_0 = i\kappa_0$ defined such that $\Omega(\kappa) = \sqrt{\kappa \tan \kappa}$ and $\Omega' = X/T$. Note that $(0 < \kappa_0 < \pi/2)$. After writing (25) in the form

$$F(X, V) = \mathrm{Im} \int_0^{\infty} \frac{\omega}{\sinh 2k} \cosh kV \left(e^{i\omega t} - e^{-i\omega t}\right) H_0^{(1)}(kX) dk \qquad (34)$$

the contour of integration may be deformed to pass up the imaginary axis, from 0 to $i\kappa_0$, and then parallel to the real axis to $k = \infty + i\kappa_0$. The integral along the imaginary axis is real and does not contribute to (34). For the integral parallel to the real axis the asymptotic expansion (18) may be used for the Hankel function, confirming that the lower limit of this integral is a saddle point and the path of steepest descent is orthogonal to the imaginary axis. It follows that

$$F(X,V) \simeq \sqrt{\frac{\tan\kappa_0}{\Omega_0'' XT}} \frac{\cos\kappa_0 V}{\sin 2\kappa_0} \exp(\Omega_0 T - \kappa_0 X) \tag{35}$$

The difference between the oscillatory and exponential behaviour is obvious in (33) and (35). It should be noted that the slowly-varying component (29) is present only behind the front. Higher-order terms in (35) can be derived in a manner analogous to (33).

It remains to consider the transition region near the front, where $X \simeq T >> 1$. In this case the saddle point approaches the origin $k = 0$, and asymptotic expansion of the Bessel function is not justified. In the vicinity of $k = 0$ the dispersion relation is approximated by

$$\omega = k - \frac{k^3}{6} + O(k^5)$$

Using the new integration variable $u = \sinh^{-1}(k)$, and expanding the integrand about $u = 0$, it follows that

$$F = \int_0 \left[1 - \tfrac{1}{3}u^2 + \tfrac{1}{2}u^2V^2 + O(u^4)\right] \sin\left(uT + O(u^5T)\right) J_0(X\sinh u)du \tag{36}$$

The leading-order contribution

$$F \simeq \int_0^\infty \sin(uT) J_0(X\sinh u)du = \frac{1}{\pi}\sinh(\tfrac{\pi}{2}T)\left[K_{\frac{1}{2}iT}(\tfrac{1}{2}X)\right]^2 \tag{37}$$

is evaluated from a variant of Nicholson's integral (Erdélyi, *et al*, 1954, §2.13, eq. 58), where K denotes the modified Hankel function of imaginary order $\frac{1}{2}iT$. The next term in the asymptotic expansion of F, associated with the $O(u^2)$ terms in (36), can be evaluated from the second derivative of (37) with respect to T. This procedure may be extended to include terms of higher order.

A uniform asymptotic expansion of the modified Hankel function in (37) has been derived in the transition region by Balogh (1967). In the form given by Olver (1974, p. 425) the leading term is

$$K_{i\nu}(\nu z) \simeq \pi\nu^{-\frac{1}{3}} e^{-\nu\pi/2} \left(\frac{4\zeta}{1-z^2}\right)^{\frac{1}{4}} \mathrm{Ai}\left(-\nu^{\frac{2}{3}}\zeta\right)$$

where Ai is the Airy integral and the parameter ς is defined by

$$\tfrac{2}{3}\varsigma^{\frac{3}{2}} = \log\left(\frac{1+\sqrt{1-z^2}}{z}\right) - \sqrt{1-z^2} = \tfrac{1}{3}(1-z^2)^{\frac{3}{2}} + O(1-z^2)^{\frac{5}{2}}$$

In the present case $\nu = \frac{1}{2}T$ and $z = X/T$. With these substitutions in (37) it follows that

$$F \simeq 2^{\frac{1}{3}}\pi T^{-\frac{2}{3}}\left[\mathrm{Ai}\left(-(\tfrac{1}{4}\mathrm{T})^{\frac{2}{3}}(1-\mathrm{X}^2/\mathrm{T}^2)\right)\right]^2 \tag{38}$$

If the asymptotic expansions of the Airy integral are used, for large negative or positive values of its argument, (38) can be shown to overlap with the corresponding approximations of (32) plus (33), or (35), respectively, for small values of k_0 or κ_0. Higher-order terms can be obtained by use of the complete asymptotic expansion of the modified Hankel function (Olver, 1974, p. 425), and the procedure outlined following (37).

It is interesting to note that the square of an Airy function is involved here, giving rise to both oscillatory and slowly-varying components in a similar manner to the infinite-depth limit discussed in §6. This feature of the far-field wave motion differs from the analogous two-dimensional case, where the Airy function enters in a linear manner and the slowly-varying component is absent (Whitham, 1974).

Some computational results are shown in Figures 1-2 and Table 4 for the function $\Phi(X,T) = F(X,2,T) + F(X,0,T)$, equivalent to the nondimensionalized source potential (22) when the source and field points are both in the free surface and $t > 0$. The computations are based on numerical integration of the difference between (25) and the infinite-depth integral F_∞. Figure 1 shows a sequence of 'snapshots' for $T = 1, 2, 3, ..., 16$. The advance of the front with unit velocity is apparent, as is the absence of waves ahead of the front. The short-wavelength oscillations for small values of X are an obvious feature. Figure 2 shows the difference $\Phi - \Phi_\infty$, where the short waves are effectively removed.

On a historical note, Rayleigh (1909) considered the solution of the two-dimensional Cauchy-Poisson problem in both finite and infinite depth, and contrasted the far-field asymptotic behaviour of the two cases. The closing paragraph in that work is noteworthy:

> If we attempt to fill up the gaps in our solution by applying quadratures ... we have to face the difficulty that, as written, the integral is not convergent. Some analytical transformation is called for. One way out of the difficulty might be to calculate the difference between the solutions for finite and infinite depth, for it would appear that the nonconvergent part of the integral, corresponding to infinitely small wavelengths, must be the same for both.

Table 4 lists the computational results for $T = 10$, as well as the corresponding asymptotic approximations derived from the leading term of (32) plus (33) for points behind the front, from (35) ahead of the front, and from (38) near the front. From comparison of the last three columns it is apparent that the asymptotic approximations are qualitatively correct, but more complete asymptotic expansions are required for numerical purposes.

X	$\Phi - \Phi_\infty$	Φ_∞	Φ	Φ_A	(38)
1	0.208058	-1.809516	-1.601458	-1.771233	0.184112
2	0.255121	-0.206861	0.048260	-0.132532	0.216880
3	0.135583	1.375727	1.511310	1.413654	0.271550
4	-0.110938	-0.018690	-0.129628	-0.199518	0.343613
5	0.301172	-0.545149	-0.243976	-0.369075	0.419613
6	0.769164	-0.348449	0.420715	0.282065	0.476037
7	0.809345	-0.135816	0.673529	0.563328	0.486309
8	0.576039	-0.011280	0.564759	0.506230	0.435689
9	0.311478	0.048964	0.360443	0.386268	0.334335
10	0.122172	0.073451	0.195623		0.214972
11	0.015176	0.079871	0.095048	0.147248	0.113402
12	-0.035201	0.077758	0.042557	0.055907	0.048079
13	-0.054106	0.071988	0.017882	0.021917	0.016053
14	-0.057846	0.064986	0.007139	0.008422	0.004137
15	-0.055178	0.057910	0.002732	0.003146	0.000806
16	-0.050274	0.051283	0.001009	0.001142	0.000117
17	-0.044942	0.045303	0.000361	0.000404	0.000012
18	-0.039888	0.040014	0.000126	0.000140	0.000001
19	-0.035342	0.035385	0.000043	0.000047	0.000000
20	-0.031340	0.031354	0.000014	0.000016	0.000000

Table 4 – Values of the difference integral, infinite-depth component, and total finite-depth potential $\Phi(X,T) = F(X,2,T) + F(X,0,T)$ for $T = 10$. The source and field points are both in the free surface. Φ_A denotes the asymptotic approximation evaluated behind the front $X = T$ from the leading term in (32) plus (33), and ahead of the front from (35). The last column, evaluated from (38), is the asymptotic approximation valid near the front.

8. Discussion and conclusions

Several examples have been given to show the utility of multivariate polynomial approximations in the evaluation of free-surface Green functions. The algorithms described have lead to substantial reductions in computing time, particularly on vector computers where the systematic use of polynomials with the same form in different subdomains of the computational space permits the simultaneous evaluation of a large array of Green functions within a single vectorized loop.

The use of economized polynomials is effective for evaluating those components of the Green functions which are slowly-varying. Analysis is required to develop suitable forms for representing singular features, as in the simpler case of a typical special function such as the Bessel functions. Appropriate forms for this purpose have been indicated in §§4-6. For the finite-depth transient Green function, the large-time asymptotic analysis in §7 is expected to serve as the basis for efficient numerical approximations, but that extension is left for future work.

An alternative to the use of polynomial approximations is to interpolate in a precomputed table. The later technique has been utilized for the infinite-depth Green functions by Delhommeau (1989) in the frequency domain, and Ferrant (1988) and Magee & Beck (1989) in the time domain. Large tables are required in these works, ranging from 64,000 to 2,000,000 entries. Thus the memory requirements are greater, and substantial time may be involved in table look-up. Comparisons of computing time are difficult to resolve due to differences in the accuracy achieved, and in the computing systems used.

There is of course a fundamental similarity between interpolation in a table and the alternative use of economized polynomials. In the most extreme case, where the number of subdomains is sufficiently large to permit the use of economized polynomials of degree one, the result is practically equivalent to linear interpolation in a table. Similarly, if some quadratic terms are included, the resulting algorithm is closely related to the bicubic interpolation scheme of Magee & Beck (1989). In both cases there is a minor advantage for the economized polynomial in that it approximates to a minimax fit, but that feature is not important at such a low degree. The most important advantages of the economized polynomial appear to be (a) that it permits a wide option of choices compromising between subdivision of the computational domain and the degree of the polynomials; and (b) that when the polynomial degree is substantial the minimax approximation increases the computational efficiency.

In the examples described here polynomials of maximum degree 5-10 have been used, with $O(100)$ subdivisions of the computational domain. These choices have been based at least in part on the desire to restrict the total number of polynomial coefficients to a few thousand, and we have not systematically studied the effect on computing efficiency of substantially larger numbers of subdivisions with simpler polynomials in each one. Such a comparison obviously would depend on the particular computing system utilized, more specifically on the relative speed of floating-point operations *vs.* random access to memory.

The free-surface Green functions are more difficult to evaluate when a uniform horizontal translation is imposed to account for the forward velocity of a ship. Since the

flow is not axisymmetric, an additional coordinate is required in approximations or tables. A more fundamental difficulty is the existence of an essential singularity downstream in the plane of the free surface, when the source point is in the same plane. Finally, it is difficult to derive asymptotic expansions in the far field with uniform accuracy, particularly near the outer limits of the Kelvin wave system. The Green function consists of two distinct components, a double integral which is symmetric about the axis of translation and evanescent, and a single integral which describes the wavelike features downstream. The double integral appears superficially to be more difficult to evaluate, but in fact the converse is the case. Effective triple polynomials for evaluating the double integral have been tabulated by Newman (1987). For the single integral Neumann expansions originally derived by Bessho are effective in part of the computational domain (Baar & Price, 1988), but not far downstream or close to the essential singularity on the axis. These difficult domains are discussed by Ursell (1960, 1988), Newman (1988) and Clarisse (1989, 1990). The generalization where oscillatory time-dependence is superposed with uniform translation is considered by Ohkusu & Iwashita (1989), using a numerical implementation of the method of steepest descent.

The mathematical difficulties which result from a steady forward velocity can be circumvented by analysing the moving steady-state source as a sequence of impulsive Green functions, in essentially the same manner that Kelvin originally analysed ship waves. The Green functions considered in §§6-7 are applicable, provided the computations can be performed over a sufficient time to reach a steady state. Numerical examples for a point source are given by Newman (1985b), and substantial progress using this approach has been made by King *et al* (1988).

In two distinct areas free-surface Green functions have been abandoned in favour of distributions of Rankine singularities on the free surface. The first is the numerical solution of fully-nonlinear wave/body problems in the time domain, where impressive progress has been made by several workers in the past decade. However these solutions are for idealized bodies, primarily in two dimensions, and applications for general bodies in three dimensions appear at present to be impractical. The second area is the analysis of three-dimensional steady-state ship waves and wave resistance, based on the method originally developed by Dawson. Here practical results have been achieved, and recent efforts have been made to extend this approach to oscillatory motions in waves. There are fundamental limitations on the ability of this method to compute waves in the far field, and to solve the oscillatory problem in the low-frequency regime where waves are radiated upstream. In both areas there are potential advantages in hybrid solutions, combining Rankine distributions in the near field with free-surface Green functions on an exterior matching boundary.

The numerical analysis of free-surface Green functions is challenging from the complementary viewpoints of classical analysis, asymptotics, and approximation theory. The results obtained in recent years have facilitated the hydrodynamic analysis of offshore platforms. More work remains, particularly in the case where uniform translation is involved, but the possibility of robust panel methods for analysing moving ships seems much closer to a reality than was true a few years ago.

Acknowledgement

Portions of this work have been supported by the Office of Naval Research, the Exxon Production Research Company, and by a Joint Industry Project which includes sponsorship from Det norske Veritas, Norsk Hydro AS, Shell Development Company and Statoil AS.

References

Abramowitz, M., & Stegun, I. A., 1964 *Handbook of Mathematical Functions with Formulas, Graphs, and Mathematical Tables*, Government Printing Office, Washington and Dover, New York.

Baar, J. J. M. & Price, W. G., 1988 Evaluation of the wavelike disturbance in the Kelvin wave source potential, *J. Ship Research* **32**, 1, 44-53.

Balogh, C. B., 1967 Asymptotic expansions of the modified Bessel function of the third kind of imaginary order. *SIAM J. Appl. Math.* **15**, 1315-1323.

Breit, S. R., 1990 The potential of a Rankine source between parallel planes and in a rectangular cylinder, unpublished manuscript.

Chester, C., Friedman, B., & Ursell, F., 1957 An extension of the method of steepest descents, *Proc. Camb. Phil. Soc.* **53**, 599-611.

Clarisse, J. M., 1989 On the numerical evaluation of the Neumann-Kelvin Green function, M.S. Thesis, MIT, Cambridge, MA.

Clarisse, J. M., 1990 Thirty years after... the evaluation of the single integral part of the Kelvin wave source potential in the far-field. Fifth International Workshop on Water Waves and Floating Bodies, Manchester.

Delhommeau, G., 1989 Amélioration des performances des codes de calcul de diffraction-radiation au premier ordre. 2èmes Journées de l'Hydrodynamique, Nantes.

Erdélyi, A., Magnus, W., Oberhettinger, F., & Tricomi, F. G., 1954 *Tables of integral transforms*, 1, McGraw-Hill, New York.

Ferrant, P. 1988 Radiation d'ondes de gravité par les mouvements de grande amplitude d'un corps immergé. Thèse de Doctorat, Université de Nantes.

Gradshteyn, I. S. & Ryzhik, I. M. 1965 *Tables of Integrals, Series and Products*, Academic Press, New York.

Havelock, T. H. 1955 Waves due to a floating sphere making periodic heaving oscillations, *Proc. Roy. Soc.* A, **231**, 1-7.

King, B. K., Beck, R. F. & Magee, A. R. 1988 Seakeeping calculations with forward speed using time-domain analysis. 17th Symposium on Naval Hydrodynamics, The Hague.

Magee, A. R. & Beck, R. F. 1989 Vectorized computation of the time-domain Green function. Fourth International Workshop on Water Waves and Floating Bodies, Øystese, Norway.

Newman, J. N. 1985a Algorithms for the free-surface Green function, *Journal of Engineering Mathematics*, **19**, 57-67.

Newman, J. N. 1985b The evaluation of free-surface Green functions, Fourth International Conference on Numerical Ship Hydrodynamics, Washington.

Newman, J. N. 1987 Evaluation of the wave-resistance Green function - Part 1 - The double integral, *Journal of Ship Research*, **31**, 2.

Newman, J. N. 1988 Evaluation of the wave-resistance Green function near the singular axis, Third International Workshop on Water Waves and Floating Bodies, Woods Hole.

Ohkūsu, M. & Iwashita, H. 1989 Evaluation of the Green function for ship motions at forward speed and application to radiation and diffraction problems, Fourth International Workshop on Water Waves and Floating Bodies, Øystese, Norway.

Olver, F. W. J., 1974 *Asymptotics and special functions*, Academic Press, New York.

Rayleigh, Lord 1909 On the instantaneous propagation of disturbance in a dispersive medium, exemplified by waves on water deep and shallow, *Phil. Mag.*, Series 6, **18**, 1-6.

Ursell, F. 1949 On the heaving motion of a circular cylinder on the surface of a fluid, *Quart. J. Mech. Appl. Mech.* **2**, 218-31.

Ursell, F. 1960 On Kelvin's ship-wave pattern, *J. Fluid Mech.* **8**, 418-31.

Ursell, F. 1988 On the Kelvin wave-source potential, Third International Workshop on Water Waves and Floating Bodies, Woods Hole.

Wehausen, J. V. & Laitone, E. V. 1960 Surface waves, *Handbuch der Physik*, **9**, 446-778. Springer-Verlag, Berlin.

Whitham, G. B. 1974 *Linear and Nonlinear Waves*, Wiley-Interscience, New York.

Appendix – extension of equation 33

An algorithm for extending (33) to higher-order terms can be constructed for $T >> 1$ in a manner analogous to (20). It is convenient to define $\omega_n = [d^n/dk^n\,\omega(k)]_{k=k_0}$. Note that $\omega_1 \equiv \omega_0'$ is positive, decreasing monotonically from 1 to 0 as k increases along the positive real axis, and $\omega_2 \equiv \omega_0''$ is negative. For $X/T = O(1)$ $k_0 = O(1)$ whereas if $X/T << 1$ $k_0 \simeq (T/2X)^2$. Thus for all values of $0 < X < T$ the product $k_0 X >> 1$, and the asymptotic expansion (18) may be used near the saddle point. After making this substitution,

$$f_2 \simeq -i\sqrt{\frac{2}{\pi X}}e^{i\pi/4}\sum_{n=0}(-i)^n c_n X^{-n}\int_{i\kappa_0}^{\infty}\frac{\omega}{\sinh 2k}\cosh kV e^{i\omega T - ikX}(k)^{-n-\frac{1}{2}}dk$$

$$\equiv -i\sqrt{\frac{2}{\pi X}}e^{i\pi/4}\sum_{n=0}(-i)^n c_n X^{-n}\int_{i\kappa_0}^{\infty}\lambda_n(k)e^{i\omega T - ikX}dk \qquad (A1)$$

To expand the last integral, we first define a local variable $u = e^{i\pi/4}(k - k_0)$, together with the Taylor series expansion

$$i\omega(k)T - ikX = i\omega_0 T - ik_0 X + iT\sum_{m=2}\frac{\omega_m}{m!}u^m e^{-im\pi/4}$$

and define the new variable v such that

$$i\sum_{m=2}\frac{\omega_m}{m!}u^m e^{-im\pi/4} = -\frac{1}{2}|\omega_2|v^2$$

Thus

$$v = \sum_{m=0} a_m u^{m+1} e^{-im\pi/4}$$

where $a_0 = 1$. Reverting the last series gives a relation for $u(v)$ in the form

$$u = \sum_{m=0} b_m v^{m+1} e^{-im\pi/4}$$

where $b_0 = 1$. The first three coefficients in these series are defined as follows:

$$a_0 = 1$$
$$a_1 = \frac{1}{6}(\omega_3/\omega_2)$$
$$a_2 = \frac{1}{24}(\omega_4/\omega_2) - \frac{1}{72}(\omega_3/\omega_2)^2$$

$$b_0 = 1$$
$$b_1 = -a_1 = -\frac{1}{6}(\omega_3/\omega_2)$$
$$b_2 = 2a_1^2 - a_2 = \frac{5}{72}(\omega_3/\omega_2)^2 - \frac{1}{24}(\omega_4/\omega_2)$$

The last integral in (A1) can be expanded in the form

$$\int_{i\kappa_0}^{\infty} \lambda_n(k) e^{i\omega T - ikX}\, dk$$

$$\simeq e^{i\omega_0 T - ik_0 X} \int_{-\infty}^{\infty} \frac{\lambda_n(k)}{dv/dk} \exp(-\frac{1}{2}|\omega_2|Tv^2)dv$$

$$= e^{i\omega_0 T - ik_0 X - i\pi/4} \int_{-\infty}^{\infty} \sum_{m=0} d_n^m v^m e^{-im\pi/4} \exp(-\frac{1}{2}|\omega_2|Tv^2)dv \qquad (A2)$$

$$= e^{i\omega_0 T - ik_0 X - i\pi/4} \sqrt{\frac{2\pi}{|\omega_2|T}} \sum_{m=0} d_n^{2m} \frac{(2m-1)!!}{(|\omega_2|T)^m} e^{-im\pi/4}$$

where $(2m-1)!! = (2m-1)\cdot(2m-3)\cdot\ldots\cdot 3\cdot 1$, and the coefficients d_n^m are defined by the series

$$\lambda_n(k)\frac{du}{dv} = \sum_{m=0} d_n^m v^m e^{-im\pi/4}$$

Substitution of (A2) in (A1) gives the desired asymptotic expansion

$$f_2 \simeq -2ie^{i\omega_0 T - ik_0 X} \sqrt{\frac{1}{|\omega_2|XT}} \sum_{n=0} (-i)^n c_n X^{-n} \sum_{m=0} d_n^{2m} \frac{(2m-1)!!}{(|\omega_2|T)^m} e^{-im\pi/4} \qquad (A3)$$

In the limit where $X/T \to 0$, $k_0 \to \infty$ and (A3) is equivalent to the infinite-depth expansion (18).

The term in (A3) with $m = n = 0$ is equal to (33). Higher-order terms can be evaluated in principle, but the algebra is cumbersome for $m > 0$. The two terms $(m = 0, n = 1)$ and $(m = 1, n = 0)$, which are of comparable order, require the coefficients

$$d_1^0 = \lambda_1(k_0) = \frac{\omega_0}{\sinh 2k_0} \cosh(k_0 V)(k_0)^{-\frac{1}{2}}$$

and

$$d_0^2 = \tfrac{1}{2}\lambda_0'' + 3b_1\lambda_0' + 3b_2\lambda_0$$

where primes denote differentiation with respect to the variable k_0. Expressions for evaluating these derivatives are given below.

$$\lambda_0 = \frac{\cosh(k_0 V)}{\sinh(2k_0)} \omega_0 k_0^{-\frac{1}{2}}$$

$$\lambda_0' = \frac{\cosh(k_0 V)}{\sinh(2k_0)} \left(\omega_1 k_0^{-\frac{1}{2}} - 2\coth(2k_0)\omega_0 k_0^{-\frac{1}{2}} - \tfrac{1}{2}\omega_0 k_0^{-\frac{3}{2}} \right) + \frac{\sinh(k_0 V)}{\sinh(2k_0)} \omega_0 V k_0^{-\frac{1}{2}}$$

$$\lambda_0'' = \frac{\cosh(k_0 V)}{\sinh(2k_0)} \left(-4\omega_0 k_0^{-\frac{1}{2}} + \omega_0 V^2 k_0^{-\frac{1}{2}} + \tfrac{3}{4}\omega_0 k_0^{-\frac{5}{2}} - \omega_1 k_0^{-\frac{3}{2}} + \omega_2 k_0^{-\frac{1}{2}} \right.$$

$$\left. + \coth(2k_0)(2\omega_0 k_0^{-\frac{3}{2}} - 4\omega_1 k_0^{-\frac{1}{2}}) + 8\coth^2(2k_0)\omega_0 k_0^{-\frac{1}{2}} \right)$$

$$+ \frac{\sinh(k_0 V)}{\sinh(2k_0)} V \left(-\omega_0 k_0^{-\frac{3}{2}} + 2\omega_1 k_0^{-\frac{1}{2}} - 4\coth(2k_0)\omega_0 k_0^{-\frac{1}{2}} \right)$$

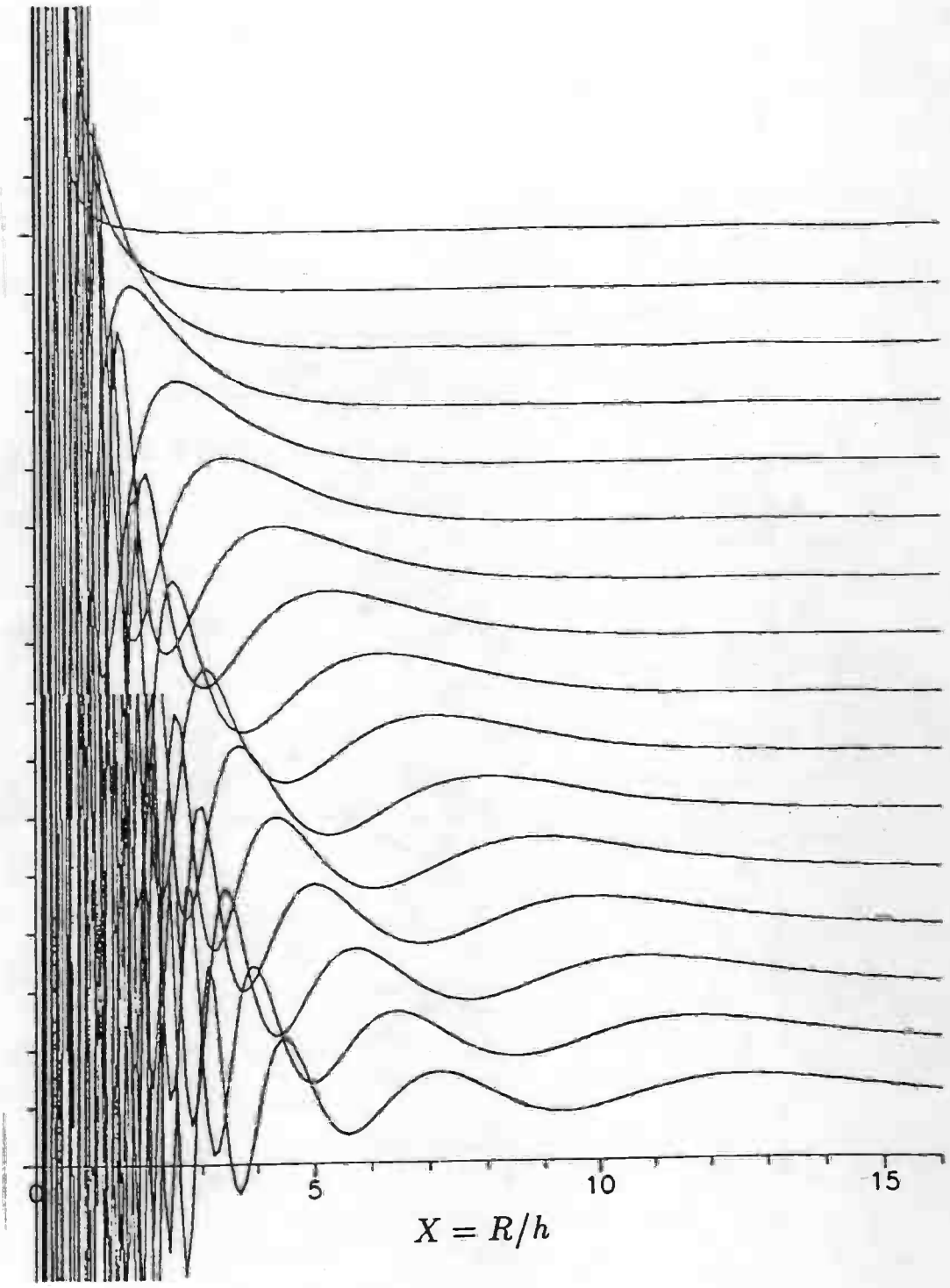

Figure 1 - Sequence of values of the source potential (22) for nondimensional times $t\sqrt{g/h} = 1, 2, \ldots, 16$. Each successive curve is displaced downward by a unit increment to indicate the progressive front.

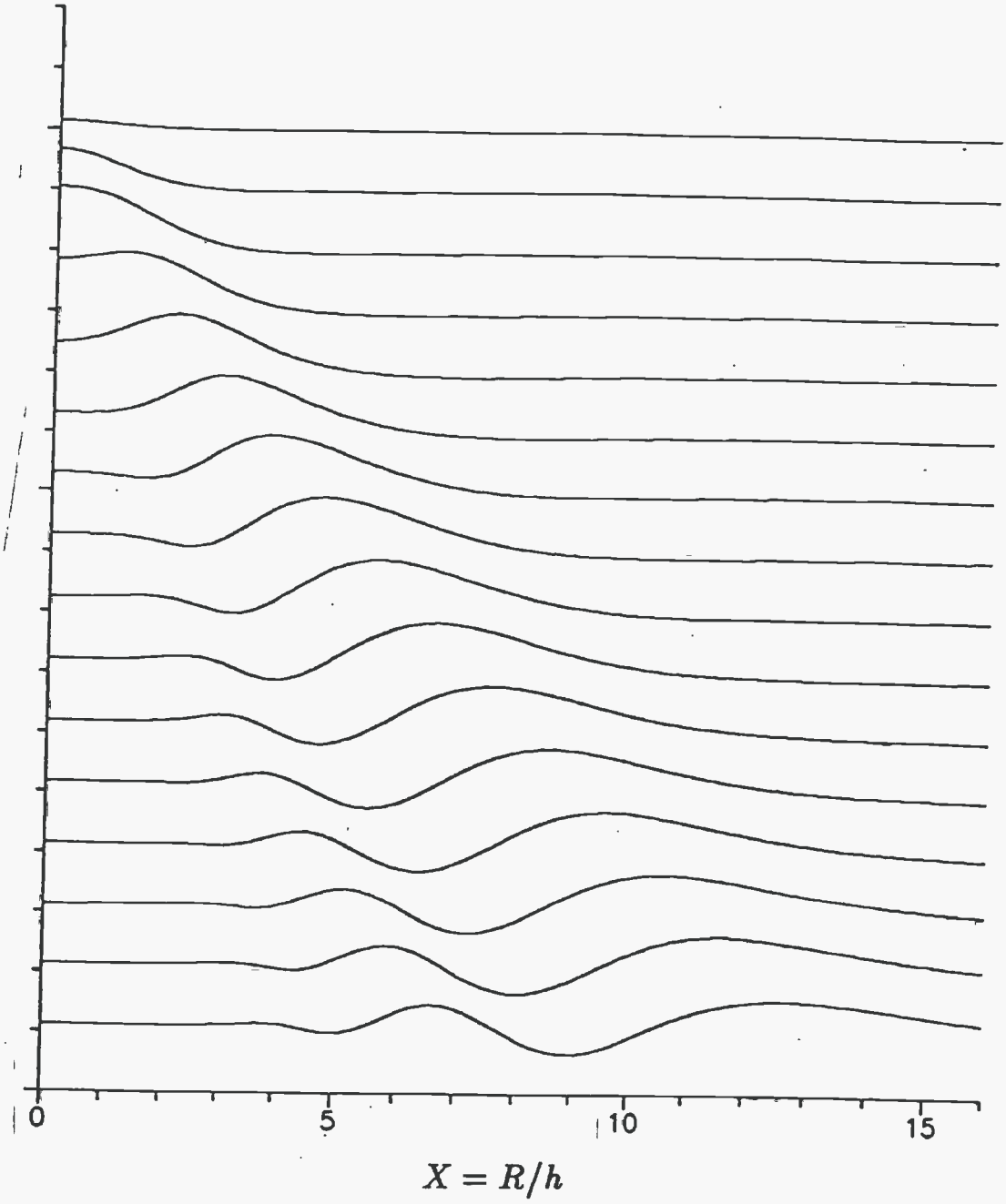

Figure 2 - Sequence of values of the difference (finite-minus infinite-depth) source potential for nondimensional times $t\sqrt{g/h} = 1, 2, \ldots, 16$. (cf. Figure 1).